

Parameter dependence of stochastic resonance in the stochastic Hodgkin-Huxley neuron

Sang-Gui Lee and Seunghwan Kim

*Brain Research Center and Nonlinear and Complex Systems Laboratory, Department of Physics and Mathematics,
Pohang University of Science and Technology, San 31 Hyojadong, Pohang 790-784, Korea*

(Received 26 January 1998; revised manuscript received 16 February 1999)

Recently, the phenomena of stochastic resonance (SR) have attracted much attention in the studies of the excitable systems under inherent noise, in particular, nervous systems. We study SR in a stochastic Hodgkin-Huxley neuron under Ornstein-Uhlenbeck noise and periodic stimulus, focusing on the dependence of properties of SR on stimulus parameters. We find that the dependence of the critical forcing amplitude on the frequency of the periodic stimulus shows a bell-shaped structure with a minimum at the stimulus frequency, which is quite different from the monotonous dependence observed in the bistable system at a small frequency range. The frequency dependence of the critical forcing amplitude is explained in connection with the firing onset bifurcation curve of the Hodgkin-Huxley neuron in the deterministic situation. The optimal noise intensity for maximal amplification is also found to show a similar structure. [S1063-651X(99)03407-8]

PACS number(s): 87.10.+e, 05.40.-a

In the last decades, the phenomena of stochastic resonance (SR) [1] have attracted much attention [2,3] in the studies of noisy systems including recent works on coherence resonance [4], which is a SR-like resonance in the system without periodic signal. Biological systems including excitable nervous systems have been much studied both theoretically [5–7] and experimentally [8,9] because they constitute one of the most important systems showing SR phenomena due to the high nonlinearity in their dynamical responses and large inherent noise. Among them, sensory nervous systems have drawn much attention since stochastic neural dynamics is proposed to play a key role in the sensing mechanism of detecting faint, information-bearing signals traveling through noisy environments [9]. Much of theoretical works have been done to explain this sensing mechanism through studies of various neural systems [5–7].

SR phenomena arise in nonlinear stochastic systems, some of which possess an inherent natural frequency. A typical example of the nonlinear system with a natural frequency is provided by the models of neurons, while that without a natural frequency, the bistable system. In the case of the bistable system with the standard double-well potential, Jung and Hänggi studied SR as a function of the forcing amplitude [10]. At a small frequency range, they observed the existence of a critical forcing amplitude where the resonance phenomena disappears. They found that this critical forcing amplitude corresponds to the parameter where the deterministic system makes a transition from nonswitching dynamics to switching dynamics. In this study, they also found that the optimal noise intensity with maximal amplification of the signal increases monotonically as the stimulus frequency is increased.

In this paper, we study a neural system with a natural frequency with a focus on the frequency dependence of the critical forcing amplitude and the optimal noise intensity. In this study, we use the Hodgkin-Huxley (HH) neuron, which is a paradigm for tonically spiking neurons, under a periodic stimulus and an Ornstein-Uhlenbeck (OU) noise. We find that both the critical forcing amplitude A_c and the optimal noise intensity D_{opt} show bell-shaped structures as a func-

tion of the stimulus frequency, and they become minimal near the natural frequency of the HH neuron. In fact, it is found that the bell-shaped structure of A_c as a function of the forcing frequency corresponds exactly to the firing onset bifurcation curve for the *noiseless* HH neuron under periodic stimulus only. Interestingly, we also found that the frequency dependence of the optimal noise intensity on the stimulus frequency also displays a similar bell-shaped structure with the nonmonotonic frequency dependence.

The HH neuron, which is derived from the biophysical analysis of the squid giant axon [11], shows typical dynamics of a real neuron, the spiking behavior and the refractory period, and serves as a canonical model for tonically spiking neurons based on nonlinear conductances of ion channels. This HH neuron consists of four nonlinear coupled ordinary differential equations, one for the membrane potential V and the other three for gating variables m, n, h for ion-channel dynamics,

$$\begin{aligned} \frac{dV}{dt} &= I_{ion} + I_{ext} + I_{syn}, \\ \frac{dm}{dt} &= \frac{m_{\infty}(V) - m}{\tau_m(V)}, \\ \frac{dh}{dt} &= \frac{h_{\infty}(V) - h}{\tau_h(V)}, \\ \frac{dn}{dt} &= \frac{n_{\infty}(V) - n}{\tau_n(V)}, \end{aligned} \quad (1)$$

where

$$I_{ion} = -g_{Na}m^3h(V - V_{Na}) - g_Kn^4(V - V_K) - g_l(V - V_l). \quad (2)$$

The first equation in Eq. (1) is the voltage-current relation with three kinds of currents: ionic current I_{ion} , external stimulus current I_{ext} , and synaptic current I_{syn} . The ionic current I_{ion} represents the current flow generated from the

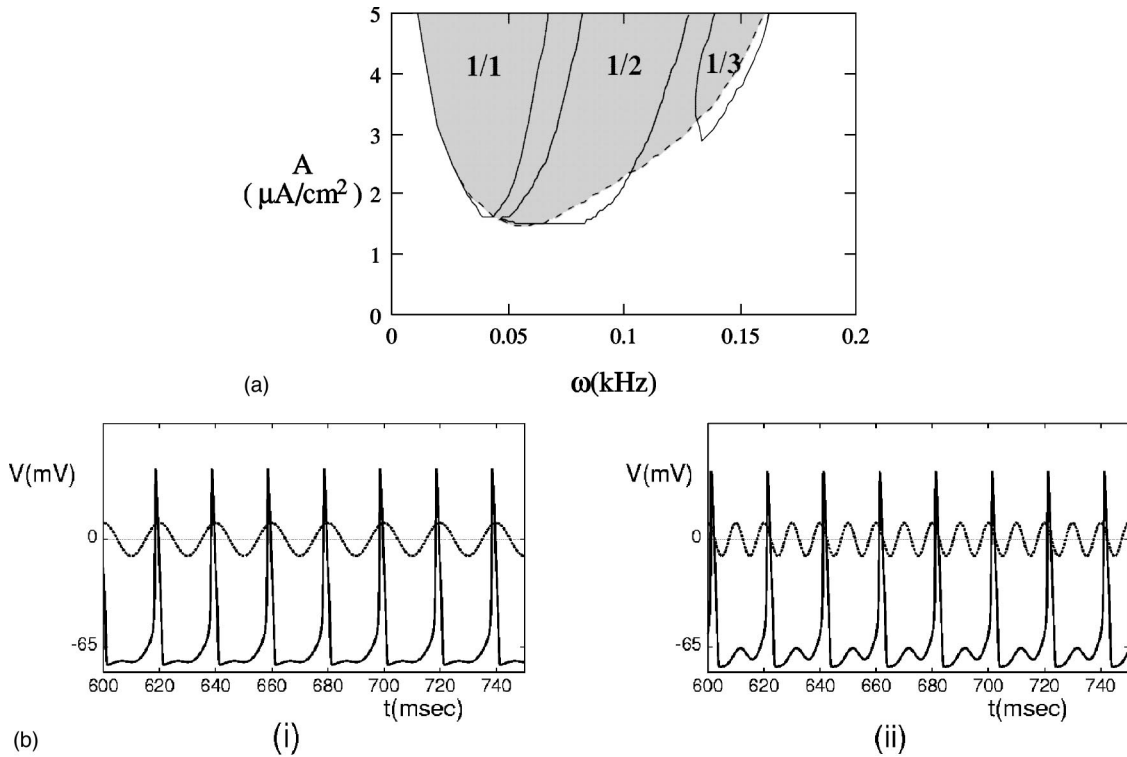


FIG. 1. (a) Phase diagram of the noiseless HH neuron under sinusoidal stimulus in the parameter space of the forcing frequency ω and the forcing amplitude A . The firing state is denoted in gray, and the nonfiring state and bistable state, in white. The dashed curve represents the firing onset bifurcation curve, and solid curves, the boundaries of mode-locking states. (b) The mode-locked membrane potential responses for $A = 5 \mu\text{A}/\text{cm}^2$ and (i) $\omega = 50 \text{ Hz}$ (1/1) and (ii) $\omega = 100 \text{ Hz}$ (1/2). The profiles of the sinusoidal stimulus currents are also superimposed in dotted curves.

ionic transport through the membrane and depends nonlinearly on the gating variables m , n , h . External stimulus current I_{ext} represents the external stimulus to a neuron, and synaptic current I_{syn} , the influence from other neurons through synaptic connections. The constants g_{Na} , g_K , and g_l are maximal conductances for sodium, potassium, and leakage currents, and V_{Na} , V_K , and V_l are corresponding reversal potentials. The parameters m_∞ , h_∞ , n_∞ , and τ_m , τ_h , τ_n represent the saturated values and the relaxation times of the gating variables m, n, h , respectively. Details on these parameter values can be found in [11–13].

In this paper we take the external stimulus to be time-dependent sinusoidal current $I_{ext}(t) = A \cos(2\pi\omega t)$, where A is the amplitude of forcing current, ω is the frequency, and t is the time in units of msec. The synaptic current I_{syn} represents the noisy component of the stimulus in a neuron from synaptic input fluctuations [14]. We model this noisy current as an additive noise from an OU process,

$$\tau_d \frac{dI_{syn}}{dt} = -I_{syn} + \sqrt{2D}\xi(t), \quad (3)$$

where $\xi(t)$ is Gaussian white noise, and D and τ_d are the noise intensity and the correlation time of the OU noise. In our numerical study, we take a typical synaptic decay time of $\tau_d = 2$ msec. Numerical integration of the HH neuron in Eq. (1) is carried out with a fourth order Runge-Kutta algorithm and that of the exponentially correlated synaptic noise in Eq. (3) with the integral algorithm proposed by Fox *et al.* [15] with an integration time step of 0.02 msec.

First we present dynamical responses of the *noiseless* HH neuron under sinusoidal current (deterministic condition) for a later comparison with the studies with noise (the stochastic condition). The phase diagram of the deterministic HH neuron in the parameter space of the forcing frequency and the forcing amplitude is shown in Fig. 1(a), which is consistent with the experimental results on the squid giant axon in [16]. In the phase diagram, parameter values for the firing state are denoted in gray, and those for the nonfiring state or the bistable region between the firing state and the nonfiring state, in white. In the firing region, mode-locking phenomena appear due to nonlinear interaction between the forcing frequency and the natural frequency of the HH neuron, which is typical in nonlinear dynamical systems with two competing periods [17]. In the mode-locked responses, the ratio between the forcing frequency and the response frequency becomes a rational. Typical mode-locked responses in the noiseless HH neuron are shown in Fig. 1(b). Note that a hierarchy of mode-locked regions with various integer ratios exist but for simplicity only the boundaries of mode-locked regions with ratios 1/1, 1/2, and 1/3, where p/q denotes p firings of spikes during q periods of the forcing current, are shown in solid lines in Fig. 1(a). Especially, the tongue-shaped boundary in a dashed curve in Fig. 1(a) separates the region with no firing from the region with firing (shaded region) as the forcing amplitude increases. This curve represents the bifurcation curve for the firing onset, which produces a bell-shaped structure as a function of the forcing frequency. Note that the forcing amplitude required for the firing onset becomes minimal near the frequency of about 55

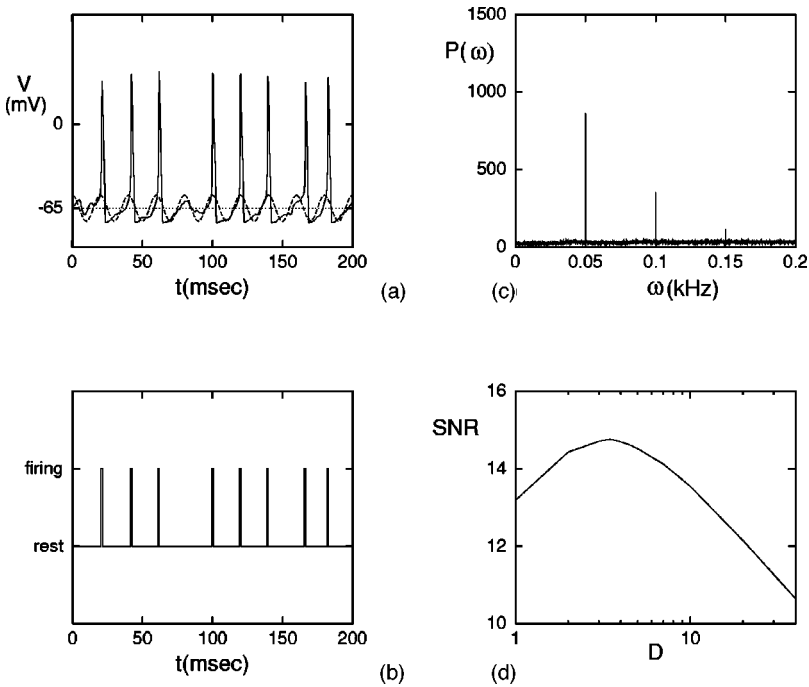


FIG. 2. Stochastic HH neuron under OU noise and periodic stimulus with $A=1.0 \mu\text{A}/\text{cm}^2$ and $\omega=0.05 \text{ kHz}$. (a) The membrane potential response for noise intensity $D=10$ is shown in a solid line and the sinusoidal stimulus current in a dashed line, (b) its spike trains, (c) the power spectrum calculated from the spike train, and (d) The SNR as a function of noise intensity D shows SR.

Hz, which is close to the natural frequency of the HH neuron observed under constant current stimuli.

A typical dynamical response of this stochastic HH neuron with the OU noise in Eq. (3) is presented in Fig. 2(a) and its spike train, a typical measure in neuroscience, in Fig. 2(b). This spike train is obtained by recording times for the generation of spikes,

$$V(t) = \sum_{i=1}^N \delta(t-t_i), \quad (4)$$

where t_i is the time at which the i th spike initiates and N is the total number of spikes in the given time interval. The power spectral density is calculated from the spike train through the fast Fourier transform as in Refs. [18,19]. This spectrum in Fig. 2(c) is characterized by broadband background noise with a signal peak at the forcing frequency ω and its higher harmonics at integer multiples of the forcing frequency. The signal-to-noise ratio (SNR) is obtained from the power spectrum as

$$R_{\text{SN}} = 10 \log_{10} \left[\frac{S(\omega)}{N(\omega)} \right], \quad (5)$$

where R_{SN} is the SNR, the signal power $S(\omega)$ is the height of the signal peak, and the noise power $N(\omega)$ is the amplitude of the background noise measured at the base of the signal peak. The obtained SNR values are plotted as a function of the noise intensity D to yield the well-established SR curve [18] in Fig. 2(d).

Now we fix the forcing frequency and study the SNR curves for various values of the forcing amplitude A . For example, we choose two forcing frequencies $\omega=0.05 \text{ kHz}$ and 0.1 kHz and show the variations of the SNR curves for

different forcing amplitudes in Fig. 3. We find that the stochastic HH neuron has a critical forcing amplitude A_c , above which the resonance with a maximal SNR disappears, similar to the bistable system. For $\omega=0.05 \text{ kHz}$, the critical

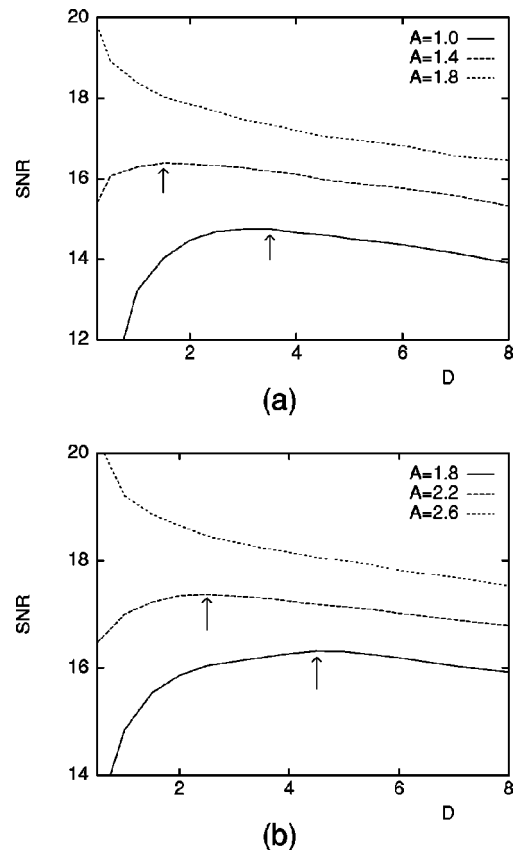


FIG. 3. The SNR curves of a stochastic HH neuron for various forcing amplitudes and forcing frequencies. (a) SNR curves for $A=1.0, 1.4, 1.8 \mu\text{A}/\text{cm}^2$ with $\omega=0.05 \text{ kHz}$. (b) SNR curves for $A=1.8, 2.2, 2.6 \mu\text{A}/\text{cm}^2$ with $\omega=0.1 \text{ kHz}$. Arrows indicate the maxima in SNR.

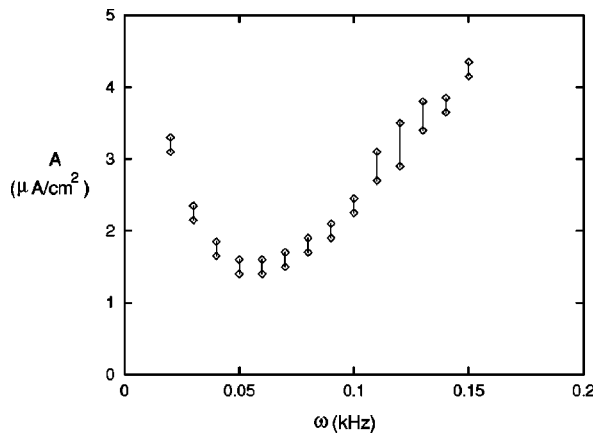


FIG. 4. Critical forcing amplitude A_c as a function of forcing frequency ω . The critical forcing amplitude lies in the solid lines.

forcing amplitude A_c is between $1.4 \mu\text{A}/\text{cm}^2$ and $1.8 \mu\text{A}/\text{cm}^2$. Note that the SNR value increases as A increases because the dynamical response of the HH neuron becomes more synchronized with stronger periodic stimulus. Similarly, for $\omega = 0.1$ kHz, the critical forcing amplitude A_c is between $2.2 \mu\text{A}/\text{cm}^2$ and $2.6 \mu\text{A}/\text{cm}^2$. This critical forcing amplitude depends strongly on the forcing frequency.

We focus our attention on the functional dependence of the critical forcing amplitude A_c on the forcing frequency ω . In the bistable system, the critical forcing amplitude increases monotonously as a function of the forcing frequency [10]. In Fig. 4, we show the dependence of A_c on the forcing frequency ω . We find for the stochastic HH neuron, as the forcing frequency increases, the critical forcing amplitude A_c decreases in the low-frequency regime but it increases in the high-frequency regime. Therefore, the dependence of A_c on ω produces a bell-shaped structure. The minimum for A_c is found to lie near the natural frequency of the system as in Fig. 4. We find that this structure for the frequency dependence of the critical forcing amplitude A_c is related to the firing onset bifurcation curve for the deterministic HH neuron shown in Fig. 1. In fact, the critical forcing amplitude curve in Fig. 4 is found to coincide with the firing onset bifurcation curve in Fig. 1(a) within error bars.

In the case of the bistable system, the critical forcing amplitude corresponds to a transition from nonswitching to switching dynamics in the deterministic condition. A nonlinear system with natural frequency, for example, the HH neuron, in the deterministic condition displays a similar dynamical transition from a nonfiring state to a firing state, where dynamics switch between the quiescent and the spiking dynamics. The firing onset bifurcation curve gives the boundary for this switching transition from the nonfiring state to the firing state. Similarly to the case of the bistable system, the critical forcing amplitude A_c in the stochastic HH neuron corresponds to the firing onset bifurcation point. The bell-shaped structure of the critical forcing amplitude and the minimality of A_c near the natural frequency of the neuron are consequences of the corresponding structure in the deterministic condition, which is due to the nonlinear resonance between the natural frequency of the HH neuron and the forc-

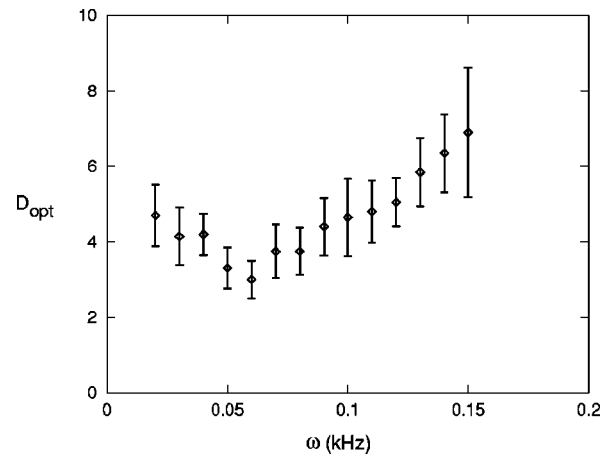


FIG. 5. Optimal noise intensity D_{opt} as a function of forcing frequency ω with a fixed forcing amplitude $A = 1.0 \mu\text{A}/\text{cm}^2$. The values of D_{opt} for various frequencies are shown with error bars calculated from five trials.

ing frequency. Note that unlike our case, the monotonous frequency dependence of the bistable system was obtained for small frequency with a narrow range [10].

Our paper shows that the analysis of the firing onset bifurcation curve in the deterministic condition provides a key to the understanding of the parameter dependence of resonance phenomena in the stochastic HH neuron. To illustrate this further, we also studied the frequency dependence of optimal noise intensity D_{opt} with fixed $A = 1.0 \mu\text{A}/\text{cm}^2$. In Fig. 5, the values of D_{opt} for various forcing frequencies are presented in the parameter space of forcing frequency ω and noise intensity D with the estimate of errorbars calculated from the five trials for each frequency. We find that D_{opt} also shows a bell-shaped structure similar to one for the critical forcing amplitude; D_{opt} becomes minimal near the forcing frequency $\omega = 0.06$ kHz close to the natural frequency of the HH neuron. As the forcing frequency moves away from $\omega = 0.06$ kHz, the required level of D_{opt} increases accordingly. The nonmonotonous frequency dependency of A_c and D_{opt} differs from that of the bistable system.

In conclusion, we have studied the parameter dependence of SR in the excitable system through the stochastic HH neuron. In particular, we have studied numerically the frequency dependence of the critical forcing amplitude A_c , above which resonance disappears, and the optimal noise intensity D_{opt} , where SNR is maximal. Our analysis of SR phenomena requires the understanding of the structure of the firing onset bifurcation curve for the deterministic system similar to the analysis of coherence resonance [4] where the understanding of the bifurcation property in the deterministic condition is also a key to the understanding of the resonance phenomena under noise. The minimal values of D_{opt} and A_c at the natural frequency of the neuron and the tongue-shaped frequency dependency of D_{opt} and A_c are understood in connection with the firing onset bifurcation curve obtained in the deterministic condition. Similar phenomena have also been found in the simulations of the stochastic FitzHugh-Nagumo neuron and are expected to hold for a large class of stochastic nonlinear systems with a natural frequency. The nonmo-

notonous dependence of D_{opt} on the forcing frequency for small forcing amplitudes is quite interesting, which probably can be understood within the framework of the linear response theory of stochastic resonance. Our results may provide a useful tip for fine tuning of SR through the control of signal parameters based on the analysis of the frequency de-

pendence of the firing onset bifurcation curve in the deterministic condition.

This work was supported by the Ministry of Education through the BSRI program (971-0202-009-2) and special fund at POSTECH. We would like to thank H. Kook and S. K. Han for stimulating discussions.

-
- [1] R. Benzi, A. Sutera, and A. Vulpiani, *J. Phys. A* **14**, L453 (1981); R. Benzi, G. Parisi, A. Sutera, and A. Vulpiani, *Tellus* **34**, 10 (1982); C. Nicolis, *ibid.* **34**, 1 (1982).
- [2] F. Moss, A. Bulsara, and M. F. Shlesinger, *J. Stat. Phys.* **70**, 1 (1993); R. Mannella and P. V. E. McClintock, *Nuovo Cimento D* **17**, 653 (1995).
- [3] F. Moss, D. Pierson, and D. O’Gorman, *Int. J. Bifurcation Chaos Appl. Sci. Eng.* **4**, 1383 (1994); K. Wiesenfeld and F. Moss, *Nature (London)* **373**, 33 (1995); A. R. Bulsara and L. Gammaitoni, *Phys. Today* **49** (3), 39 (1996); The most recent and comprehensive review: L. Gammaitoni, P. Hänggi, P. Jung, and F. Marchesoni, *Rev. Mod. Phys.* **70**, 223 (1998).
- [4] Hu Gang, T. Ditzinger, C. Z. Ning, and H. Haken, *Phys. Rev. Lett.* **71**, 807 (1993); A. S. Pikovsky and J. Kurths, *ibid.* **78**, 775 (1997); A. Longtin, *Phys. Rev. E* **55**, 868 (1997); S. G. Lee, A. Neiman, and S. Kim, *ibid.* **57**, 3292 (1998); A. Neiman, P. Saparin, and L. Stone, *ibid.* **56**, 270 (1997).
- [5] K. Wiesenfeld, D. Pierson, E. Pantazelou, C. Dames, and F. Moss, *Phys. Rev. Lett.* **72**, 2125 (1994).
- [6] A. Longtin, *J. Stat. Phys.* **70**, 309 (1993).
- [7] F. Moss, *Ber. Bunsenges. Phys. Chem.* **95**, 303 (1991).
- [8] H. A. Braun, H. Wissing, K. Schäfer, and M. C. Hirsh, *Nature (London)* **367**, 270 (1994).
- [9] J. K. Douglass, L. Wilkens, F. Pantazelou, and F. Moss, *Nature (London)* **365**, 337 (1993).
- [10] P. Jung and P. Hänggi, *Phys. Rev. A* **44**, 8032 (1991).
- [11] A. L. Hodgkin and A. F. Huxley, *J. Physiol. (London)* **117**, 500 (1952).
- [12] S. G. Lee, S. Kim, and H. Kook, *Int. J. Bifurcation Chaos Appl. Sci. Eng.* **7**, 889 (1997).
- [13] D. Hansel, G. Mato, and C. Meunier, *Europhys. Lett.* **23**, 367 (1993).
- [14] A. S. Pikovsky and J. Kurths, *Phys. Rev. Lett.* **78**, 775 (1997).
- [15] R. F. Fox, I. R. Gatland, R. Roy, and G. Vemuri, *Phys. Rev. A* **38**, 5938 (1988).
- [16] N. Takahashi, Y. Hanyu, T. Musha, R. Kubo, and G. Matsumoto, *Physica D* **43**, 318 (1990).
- [17] V. I. Arnold, *Trans. Am. Math. Soc.* **42**, 213 (1965); M. H. Jensen, T. Bohr, D. Christiansen, and P. Bak, *Solid State Commun.* **51**, 231 (1983).
- [18] A. Longtin, *Nuovo Cimento D* **17**, 835 (1995).
- [19] X. Pei, K. Bachmann, and F. Moss, *Phys. Lett. A* **206**, 61 (1995); F. Chapeau-Blondeau, X. Godivier, and N. Chambet, *Phys. Rev. E* **53**, 1273 (1996); W. J. Rappel and A. Karma, *Phys. Rev. Lett.* **77**, 3256 (1996); H. J. Kappen, *Phys. Rev. E* **55**, 5849 (1997).